An Interlinking Converter for Renewable Energy Integration into Hybrid Grids

Tang, Z.; Yang, Yongheng; Blaabjerg, F.

Published in:
IEEE Transactions on Power Electronics

DOI (link to publication from Publisher):
10.1109/TPEL.2020.3018585

Publication date:
2021

Document Version
Accepted author manuscript, peer reviewed version

An Interlinking Converter for Renewable Energy Integration into Hybrid Grids

Zhongting Tang, *Student Member, IEEE,* Yongheng Yang, *Senior Member, IEEE,* and Frede Blaabjerg, *Fellow, IEEE*

***Abstract*—This letter proposes an interlinking converter architecture, which enables flexibly integrating renewable energy into hybrid grids. The proposed converter has one AC port and two DC ports, offering a flexible solution to integrating various DC and AC sources, which can also be versatilely configured as a DC-DC converter, a DC-AC inverter, or a DC-DC/AC multiport converter. The general concept of the architecture, its common-mode voltage analysis and flexible operation modes are detailed in this letter. Experimental tests are performed on an example converter with a dedicated modulation strategy. The test results confirm the concept in terms of flexible conversion, high power density, low leakage currents as well as controllable power flow.**

***Index Terms*—Hybrid DC/AC grid, power converters, renewable energy integration, flexibility, leakage currents**

I. Introduction

RENEWABLE energy sources (RESs) like wind, photovoltaics (PV), and fuel cells are of uncertainty. The high penetration of RESs may challenge the entire power system. At present, the mixture of AC and DC grids is still the main concept to achieve a flexible, secure and reliable power supply and to accommodate more RES systems [1]. In this way, many DC generation RESs may be consumed flexibly by local loads, increasing the energy conversion efficiency and self-consumption [2], [3]. Such a hybrid grid architecture is also in alignment with the intelligent power conversion and the near-zero-energy building initiatives [4], [5].

In the prior-art research, the focus has been put on the power management and control of hybrid AC/DC grids. For instance, in [6], an overview of hybrid microgrids was presented in terms of system structures, operation modes, power management and control. The hybrid microgrid is becoming much attractive due to the increase of modern DC loads and RESs with energy storage being integrated into the system. In such applications, the interlinking converter is critical (e.g., reliability, manageability, and stability), which enables integrating various energy sources into the grid. To ensure the operation, power-sharing approaches were also developed for interlinking converters under various scenarios [6]. However, attempts to develop interlinking converters have not been intensively made in the literature, which yet can be a promising means to enhance the operation of such hybrid energy systems.

Clearly, the interlinking converter should have multiple connections (e.g., DC ports and AC ports). There are two ways to achieve so: using separated standard DC-DC and DC-AC converters to form a multistage conversion system [6] and developing stand-alone multiport configurations [7]–[13]. Compared to the former solution, standalone hybrid topologies bring more benefits (e.g., increased reliability, higher power density, and lower system cost due to the reduced number of conversion stages), and they possess more flexibility. For instance, the split-source inverters were introduced in [9] and [10] to enhance the compactness, efficiency, flexible power flow and voltage-boosting, while the leakage current issue was not considered. This is a troublesome challenge when applied in PV systems. To lower leakage currents, transformerless stand-alone converters [12], [13] can be employed, yet lacking bidirectional power flow capability. Additionally, due to adopting of a dual-buck inverter, large AC filter inductors are required, leading to a relatively low power density that contradicts with the benefits of standalone hybrid converters [12]. In all, the state-of-the-art converters have limitations when being used as an interlinking conversion stage in hybrid AC/DC grids.

In light of the above, this letter proposes an interlinking conversion architecture as a promising candidate for RES integration into hybrid grids. It has superior performance in terms of high reliability, easy implementation, and flexible operation. The proposed architecture is attained by replacing the power device of the boost converter with an active switch and a voltage source inverter (VSI), as detailed in Section II, where the pros and cons of the proposed converter are also discussed. In addition, it employs a symmetrical impedance network that is beneficial to system efficiency, leakage current suppression and power density. A dedicated modulation scheme is exemplified, which can further improve the power quality and flexible control [14], while maintaining efficiency. Experimental tests in Section III have demonstrated the efficacy of the proposed interlinking converter. Finally, concluding remarks are provided in Section IV.

II. Proposed Interlinking Converter

A. General Concept

The general concept of the proposed interlinking converter architecture for hybrid grids is shown in Fig. 1. As seen in Fig. 1, the converter has two DC ports and one AC port, where the low-voltage DC (DC_L) side can be PV panels, batteries or other RESs, and the high-voltage DC (DC_H) side can be connected to a DC grid or loads (also storages). Similarly, the AC side can be an AC load or an AC grid. Notably, all the power conversions in the proposed architecture should be bidirectional for high flexibility. To realize so, the following

Manuscript received 16 July 2020; revised 05 August 2020; accepted 18 August 2020. This work was supported by the Novo Nordisk Fonden through the Interdisciplinary Synergy Programme under Award Ref. No.: NNF18OC0034952. (Corresponding author: Yongheng Yang.)

The authors are with the Department of Energy Technology, Aalborg University, Aalborg 9220, Denmark (emails: zta@et.aau.dk, yoy@et.aau.dk, fbl@et.aau.dk).

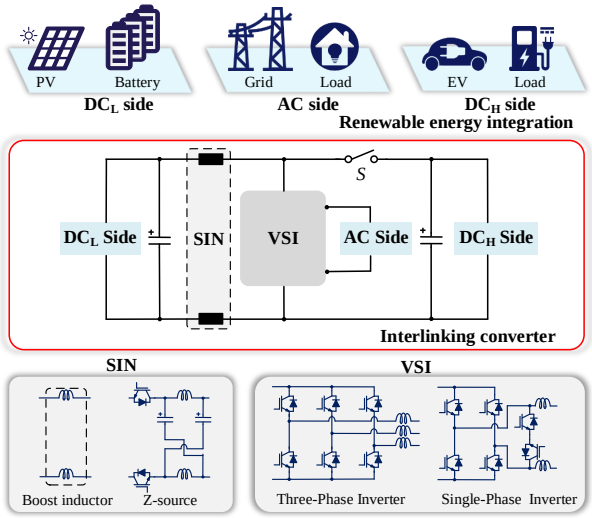

Fig. 1. General concept of the proposed interlinking converter architecture, where S represents an active switch, allowing the bidirectional power flow.

should be considered: 1) The control switch of the boost converter is replaced by a VSI with its common-mode voltage (CMV) being clamped to achieve the AC output; 2) An active switch, i.e., a synchronous rectifier switch, is adopted for the bidirectional DC-DC conversion, and accordingly, the hybrid converter can achieve boost or buck conversion between the DC_L and the DC_H sides; 3) A symmetrical impedance network (SIN) is placed at the DC_L side, as exemplified in Fig. 1, which is also essential to lower the leakage currents.

In such an architecture, the CMV will be clamped to be half of the DC_L voltage by the symmetrically arranged impedance and the VSI. To demonstrate the CMV clamping, the proposed interlinking converter architecture with a single-phase inverter is exemplified as shown in Fig. 2. As observed in Fig. 2, there are two modes, i.e., the charging and discharging states of the SIN, which are defined as follows:

(1) During the charging period, the VSI operates in shoot-though (ST) mode and the active switch S is OFF, as depicted in Fig. 2(a). Accordingly, the terminal voltages are $v_{AN} = v_{BN} = V_L/2$, and the CMV v_{cm} [12] is calculated as

$$v_{cm} = \frac{v_{AN} + v_{BN}}{2} = \frac{V_L}{2} \tag{1}$$

(2) As presented in Fig. 2(b), the SIN is discharging, the VSI operates in the DC-AC conversion mode, and S is in ON-state. Due to the CMV (denoted as v_{cmVSI}) being already clamped by the adopted VSI $v_{cmVSI} = (v_{AT}+v_{BT})/2 = V_H/2$. Considering the terminal voltage $v_{AN} = v_{AT}-V_{Z_2}$, $v_{BN} = v_{BT}-V_{Z_2}$, the resultant CMV of the proposed converter can be obtained as

$$\begin{aligned} v_{cm} &= \frac{v_{AN} + v_{BN}}{2} = \frac{(v_{AT} - V_{Z_2}) + (v_{BT} - V_{Z_2})}{2} \\ &= \frac{V_H - (V_{Z_1} + V_{Z_2})}{2} = \frac{V_L}{2} \end{aligned} \tag{2}$$

where V_{Z_1} and V_{Z_2} are the SIN voltages, i.e., $V_{Z_1} = V_{Z_2}$.

It can be observed from Eqs. (1) and (2) that the proposed interlinking conversion architecture can maintain a constant CMV due to the employment of the SIN and the VSI with its CMV being clamped. Thus, the proposed interlinking converter is suitable for PV applications. It is worth noting that the leakage current suppression can only be achieved at the DC_L side. Additional isolation equipment can be considered at the DC_H side according to application requirements (e.g., in a DC grid).

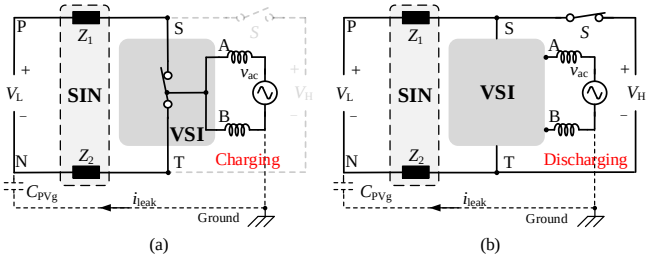

Fig. 2. Operational states of the proposed interlinking converter architecture with a single-phase inverter: (a) charging state and (b) discharging state, where Z_1 and Z_2 are the equivalent impedances of the SIN ($Z_1 = Z_2$), **P** and **N** are the positive and negative terminals of the DC_L side, **S** and **T** are the positive and negative input terminals of the VSI, **A** and **B** are the output terminals of the VSI, V_L, V_H and v_{AC} are the DC_L voltage, the DC_H voltage and the AC voltage, C_{PVg} and i_{leak} are the PV parasitic capacitor and the leakage current.

B. Operational Flexibility

As shown in Fig. 1, the adoption of the synchronous rectifier switch enables the bidirectional power flow between the DC ports. Furthermore, the VSI can also achieve reactive power injection with a dedicated modulation method, where the power factor can be adjusted between [-1, 1]. In all, the proposed hybrid converter has high flexibility and controllability for RES integration into hybrid grids. As shown in Fig. 3, the flexibility is reflected by the possible operation modes, which include: the power feed-in mode (Mode **I**), the power feed-back mode (Mode **II**), and the power factor mode (Mode **III**):

(1) In Mode **I**, the DC_L side is a source (e.g., PV panels) to provide power to the DC_H side, the AC side or both. In this case, the converter achieves the boost DC-DC conversion and DC-AC conversion from the DC_L side to the DC_H and the AC sides, respectively. Additionally, in this mode, both the DC_L and the DC_H/AC sides can feed power into the AC/DC_H side.

(2) In Mode **II**, there are three operation cases. Firstly, the power from the AC side is fed back to the DC_L and DC_H sides (i.e., the two DC ports are loads), where the converter operates in the active rectification for the DC_H side and the buck DC-DC conversion for the DC_L side from the AC side. Secondly, the power feed-back mode is the case where only the DC_L side is working as a load (e.g., charging batteries). That is, both the DC_H and AC sides are providing power. Thirdly, both the DC_L and the AC sides are acting as loads, where the DC_H side should perform the buck DC-DC and the DC-AC conversions, respectively.

(3) In Mode **III**, whatever power flow modes between the DC_L and DC_H sides are, the power factor at the AC side should be controlled flexibly to enable grid-connected applications. The proposed converter architecture can achieve so when the modulation method for the DC-AC conversion has reactive power injection capability, as indicated in Fig. 3.

When applied in a hybrid AC/DC grid (i.e., the AC and DC_H ports are connected to grids), the overall system operation can be enhanced to a large extent. For instance, when the AC grid

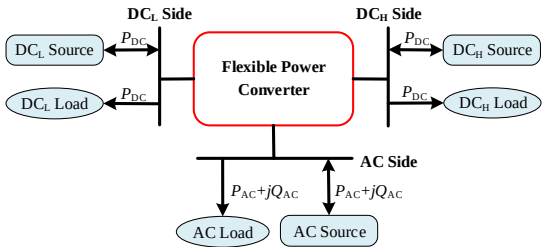

Fig. 3. Possible operation modes of the proposed interlinking conversion architecture, where P_{AC} and Q_{AC} represent the corresponding active power and reactive power at the AC port.

requires support (e.g., to tackle the frequency stability), the active power from the input DC$_L$ side can be regulated, while the DC$_H$ grid can also provide support by feeding power to the AC port. Similarly, if the DC side has stability issues under faults (e.g., under voltage issues), the AC grid can be operated in the rectification mode to help the DC grid withstand the fault. In all, the proposed power conversion architecture can be a flexible and promising solution to the integrating of RESs into hybrid AC/DC grids.

C. Topology and Modulation Example

A modulation strategy for the proposed architecture is further demonstrated on an exemplified converter using a highly efficient and reliable inverter concept (HERIC) inverter [15] as the VSI and a symmetrical inductor network as the SIN, which is shown in Fig. 4. Fig. 5 shows the modulation method for this converter. As observed in Fig. 5, this modulation scheme compares a triangular carrier m_{tri} with $1-d$ and $|m_{AC}|$, where m_{AC} is the DC-AC modulation signal. The modulation scheme is illustrated in detail as follows:

(1) When $m_{tri} \in [1-d, 1]$, the converter operates in the **ST** mode, and $S_{1\text{-}6}$ are in ON-state and S_{SR} is OFF. Moreover, the AC conversion is in zero-voltage state during this period. The CMV is clamped as half of the DC$_L$ voltage V_L by the DC inductors L_{dc1} and L_{dc2}, as discussed in Section II.A.

(2) During the period of $m_{tri} \in [0, 1-d)$, the synchronous rectifier switch S_{SR} is ON, and the HERIC adopts an improved modulation method in [14] to achieve a constant CMV (i.e., being half of V_L). In this case, $S_{1\text{-}6}$ operate following a sinusoidal pulse width modulation (PWM) scheme (i.e., by comparing m_{tri} with $|m_{AC}|$), as shown in Fig. 5.

Since the proposed interlinking conversion architecture has no **ST** protection, deadtime should be added between the switching mode transitions. The deadtime insertion is the same as that in [14]. Nevertheless, according to the above, the DC gain can be obtained as

$$\frac{V_H}{V_L} = \frac{1}{1-d} \tag{3}$$

Since the DC-DC and DC-AC conversions should be completed in one switching cycle, to avoid distortions, the followings should hold:

$$d + m_{AC} \le 1 \tag{4}$$

Accordingly, the maximum modulation signal $m_{ACmax} = 1-d$, i.e., the peak AC output voltage must satisfy:

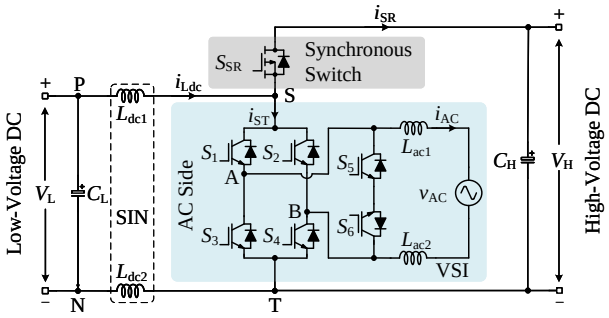

Fig. 4. An example of the proposed interlinking conversion architecture using a symmetrical boost inductor network and an HERIC, where S_{SR} is the synchronous rectifier switch, the boost inductors are L_{dc1}, L_{dc2}, (i.e., $L_{dc1} = L_{dc2}$), C_L and C_H are the DC capacitors, i_{dc}, i_{ST} and i_{SR} are the DC inductor current, the VSI input current and the synchronous rectifier switch current, i_{AC} is the current of the L-type filter (i.e., including L_{ac1} and L_{ac2}, $L_{ac1} = L_{ac2}$), and its positive direction is from the VSI to the AC grid.

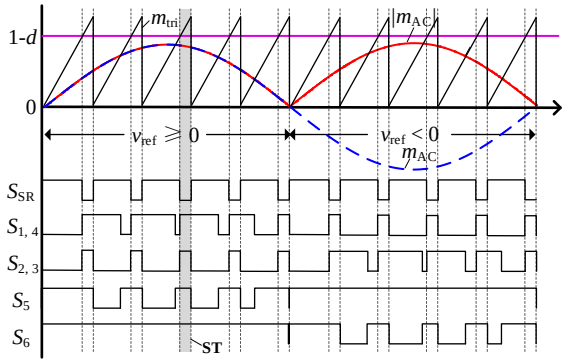

Fig. 5. A modulation scheme for the proposed converter in Fig. 4, where m_{tri} is the carrier, d is the ST interval and m_{AC} is the modulation signal of the HERIC [15].

$$V_{ACpeak} = m_{ACmax} V_H = \frac{(1-d)V_L}{(1-d)} = V_L \tag{5}$$

where V_{ACpeak} is the peak of v_{AC}. Referring to Eqs. (3) and (5), the DC-DC and the DC-AC gains of the exemplified multiport converter in Fig. 4 are the same as the conventional boost converter and the single-phase HERIC inverter, respectively.

D. Discussions

Although the proposed architecture has high flexibility, there are certain concerns in terms of conversion ratio, control and efficiency. Those can be further explored as future work to improve the performance of hybrid converters for integrating various renewable sources. When designing the system, those aspects should also be considered:

(1) *Conversion Ratio*. As shown in Eqs. (3) and (5), the conversion ratios are limited. To solve this issue, a symmetrical high-boosting impedance network [16], switched-inductor [17] or others can be adopted.

(2) *System Control*. Notably, the control of the proposed converter varies in applications. The currents are the control objectives when the ports connected to energy sources, while the voltages are controlled when the ports supplying loads. For instance, the proposed converter operates in Mode **I**, where the DC$_L$ side is the source, the DC$_H$ side is the load and the AC side is a grid. In this case, a proportional-integral

TABLE I
SYSTEM PARAMETERS OF THE POWER CONVERTER IN FIG. 4

Symbol	Parameters	Values
$V_{\rm L}$	$DC_{\rm L}$ voltage	180 V
$V_{\rm H}$	$DC_{\rm H}$ voltage	260 V
$V_{\rm AC}$	AC grid voltage (RMS)	110 V/50 Hz
$C_{\rm L}$, $C_{\rm H}$	DC capacitors	2000 uF
$L_{\rm dc1}$, $L_{\rm dc2}$	DC inductors	0.3 mH
$L_{\rm ac1}$, $L_{\rm ac2}$	L-type inductors	0.75 mH
$f_{\rm sw}$	Switching frequency	20 kHz
$C_{\rm pvg}$	PV parasitic capacitor	200 nF

(PI) controller can be adopted as the voltage control-loop for the DC-DC conversion, and a proportional-resonant (PR) controller can be used for the DC-AC conversion, respectively. In addition, due to the power coupling between the DC and AC sides, both DC ports have pulsating ripples. This is also common in conventional single-phase VSI systems, the strategies for which to mitigate the ripples may also be applied to the proposed converter. Moreover, the MPPT control of the proposed converter can be achieved flexibly, i.e., obtained in the DC-DC conversion, the DC-AC conversion or both.

(3) *Efficiency*. Comparing with the conventional two-stage system (a boost converter with an HERIC inverter), the power losses of the proposed converter are lower. Firstly, according to the modulation scheme in Fig. 5, all the full-bridge switches are used as a boost switch during the **ST** period, leading to lower switching losses of $S_{1\text{-}4}$ (i.e., the turn-ON losses of $S_{1\text{-}4}$ are eliminated in the DC-AC conversion) and lower conduction losses of $S_{\rm SR}$ (i.e., the power diode in the two-stage inverter). Therefore, the efficiency can become higher than the conventional two-stage inverter [14].

(4) *Power Density*. The proposed interlinking converter can improve the power density due to: 1) fewer power devices to obtain multiple outputs when compared to the conventional two-stage inverter; 2) smaller AC filter inductors compared to the transformerless hybrid converter with the dual-buck inverter as the VSI [12]; 3) symmetrically distributed boost inductors, resulting in lower leakage currents (thus, good power quality); 4) higher efficiency leading to a smaller heatsink, as mentioned in the above. In all, it is confirmed that the proposed converter has superior performances than the conventional two-stage solution.

III. EXPERIMENTAL RESULTS

Experimental tests are performed on a prototype, referring to Fig. 4. The power switches $S_{1\text{-}6}$ are from Infineon and the MOSFET $S_{\rm SR}$ is from Fairchild. Operation schemes and modulation algorithms are implemented in a fixed-point digital signal processor (DSP) from TI. A commercial DC source is adopted at the $DC_{\rm L}$ side. The $DC_{\rm H}$ side is supplying an ET5420 electronic load, and the AC side is connected to an AC grid. System parameters are listed in Table I. Referring to Fig. 3, Mode **I** and Mode **III** are tested.

The performance of the proposed converter in Mode **I** is shown in Fig. 6, where the $DC_{\rm L}$ side provides power to the $DC_{\rm H}$ side and the AC output. As shown in Fig. 6, the proposed architecture can provide an AC and DC outputs

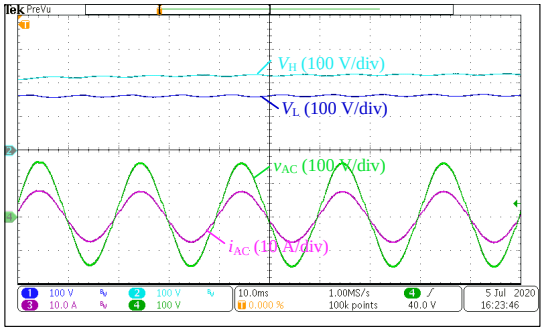

Fig. 6. Performance of the proposed interlinking converter with an HERIC as the VSI operating in Mode **I** (time: 10 ms/div).

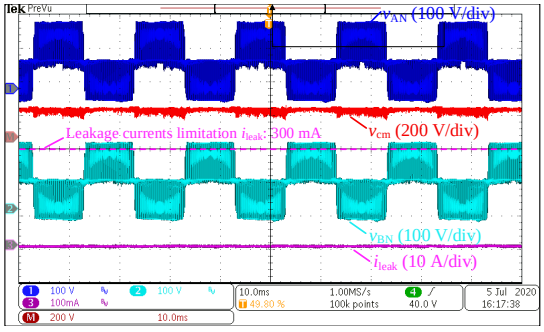

Fig. 7. Performance of the proposed converter, where $v_{\rm AN}$ and $v_{\rm BN}$ are the voltage of the terminals **A** and **B** to **N** in Fig. 4, respectively, and $v_{\rm cm}$ and $i_{\rm leak}$ are the CMV and the leakage current (time: 10 ms/div).

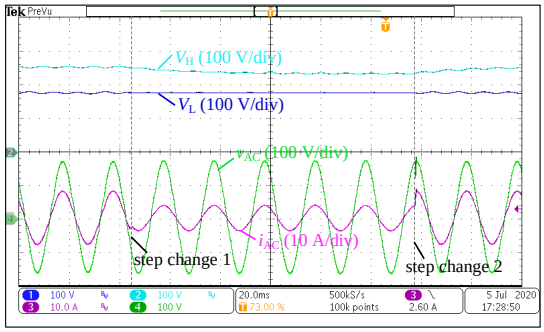

Fig. 8. Performance of the proposed interlinking converter under load step changes at the AC side in Mode **I** (time: 20 ms/div).

simultaneously. In addition, as mentioned in Section II.D, both DC voltages have ripples in Fig. 6 due to the power coupling and also the characteristics of the commercial DC source (i.e., having an internal resistance and a large output capacitor). The power decoupling strategies for the conventional VSI may also be applied to alleviate this.

Fig. 7 demonstrates the CMV and leakage currents of the proposed converter for PV applications. As shown in Fig. 7, the leakage current $i_{\rm leak}$ is below the limit (i.e., the VDE 0126) [12]. Additionally, it is illustrated by the inverter voltage $v_{\rm AN}$ and $v_{\rm BN}$ in Fig. 7 that the adopted modulation method can achieve the same performance as the HERIC with the unipolar PWM. Thus, the proposed converter can maintain low leakage currents and good power quality.

Moreover, the dynamic performance of the converter in Mode **I** has been tested under an AC load change. As shown in Fig. 8, the grid current amplitude (RMS) was changed to 2.5 A and then back to 5 A. The experimental results indicate that the proposed converter can operate stably under dynamic

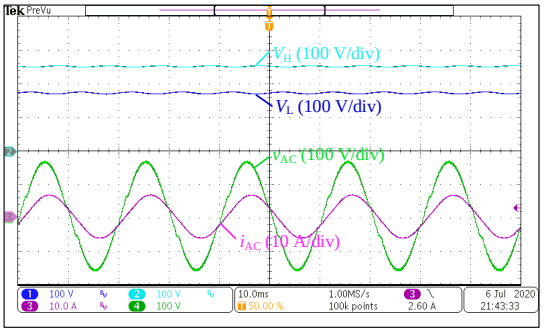

Fig. 9. Performance of the proposed interlinking converter operating in Mode **III**, where i_{AC} is lagging v_{AC} (time: 10 ms/div).

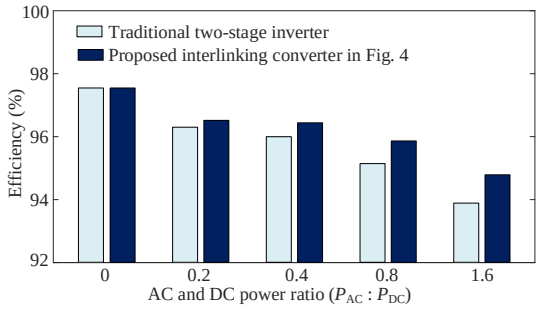

Fig. 10. Efficiency comparison of the traditional two-stage inverter and the proposed interlinking converter in Fig. 4 under different power ratios P_{AC} : P_{DC} with the total power being 1.4 kW, where P_{AC} and P_{DC} are the output power of the AC and DC_H sides.

load changes. More importantly, due to the separated control of the DC-DC and DC-AC conversions, the current quality is not affected by the load changes.

To further validate the performance of the proposed converter, experimental tests in Mode **III** are carried out and the results are shown in Fig. 9, where the DC-AC conversion operates under a non-unity power factor. Observations in Fig. 9 indicate that the proposed converter can provide flexible reactive power injection, which may be beneficial to the entire system operation (e.g., to provide grid support).

Fig. 10 presents the efficiency comparison between the traditional two-stage inverter (i.e., a boost converter and an HERIC) and the proposed converter in Fig. 4, where different AC and DC power ratios (i.e, P_{AC} : P_{DC}) are considered with the total power being 1.4 kW, and the two-stage inverter supplies a DC load at the DC-link. The conversion efficiencies, which consider the losses of the power devices and the filters, are calculated by measuring the voltages and currents of the three ports. Although the efficiency is not optimal under this power level, the results in Fig. 10 indicate that the proposed converter has a higher efficiency than the traditional two-stage inverter. Furthermore, as shown in Fig. 10, the efficiency benefit of the proposed converter will become significant when AC output power is higher (i.e., larger P_{AC} : P_{DC}), which is in agreement with the discussion in Section II.D.

In all, the above results have verified that the proposed converter can achieve flexible operation. With the dedicated modulation scheme, the proposed interlinking converter can obtain good power quality and high efficiency. Besides, when the DC_L side employs PV panels, it can achieve low leakage currents. Thus, the proposed interlinking conversion architecture provides a flexible, secure and reliable solution for future hybrid AC/DC grids with the integration of various RESs.

IV. Conclusion

In this letter, an interlinking conversion architecture was proposed as a promising solution to the integration of various energy sources into hybrid grids. The proposed architecture is implemented by replacing the power devices in the boost converter with a VSI and an active switch. The proposed interlinking conversion architecture can achieve low leakage currents, good power quality, high efficiency, and flexible power flow control. Experimental results have verified the performance of the proposed architecture. As the demand of hybrid energy systems is increasing, the flexible power conversion architecture could be a promising interlinking stage.

References

[1] I. Batarseh and K. Alluhaybi, "Emerging opportunities in distributed power electronics and battery integration," *IEEE Power Electron. Mag.*, vol. 7, no. 2, pp. 22–32, Jun. 2020.

[2] B. T. Patterson, "DC, come home: DC microgrids and the birth of the Enernet," *IEEE Power Energy Mag.*, vol. 10, no. 6, pp. 60–69, Nov. 2012.

[3] A. K. Bhattacharjee, N. Kutkut, and I. Batarseh, "Review of multiport converters for solar and energy storage integration," *IEEE Trans. on Power Electron.*, vol. 34, no. 2, pp. 1431–1445, Feb. 2019.

[4] J. Ramos-Ruiz, B. Wang, H. Chou, P. Enjeti, and L. Xie, "Power electronics intelligence at the network edge (PINE) – an approach to interface PV and battery energy storage systems at the grid edge," *IEEE J. Emerg. Sel. Top. Power Electron.*, pp. 1–1, 2020.

[5] D. D'Agostino, P. Zangheri, B. Cuniberti, D. Paci, and P. Bertoldi, "Synthesis report on the national plans for nearly zero energy buildings (NZEBs)," *EUR 27804 EN*.

[6] F. Nejabatkhah and Y. W. Li, "Overview of power management strategies of hybrid AC/DC microgrid," *IEEE Trans. Power Electron.*, vol. 30, no. 12, pp. 7072–7089, Dec. 2015.

[7] H. Ribeiro, A. Pinto, and B. Borges, "Single-stage DC-AC converter for photovoltaic systems," in *Prof. of ECCE*, Sep. 2010, pp. 604–610.

[8] A. Abdelhakim, P. Mattavelli, P. Davari, and F. Blaabjerg, "Performance evaluation of the single-phase split-source inverter using an alternative DC–AC configuration," *IEEE Trans. Ind. Electron.*, vol. 65, no. 1, pp. 363–373, Jan. 2018.

[9] S. S. Lee and Y. E. Heng, "Improved single-phase split-source inverter with hybrid quasi-sinusoidal and constant PWM," *IEEE Trans. Ind. Electron.*, vol. 64, no. 3, pp. 2024–2031, Mar. 2017.

[10] S. S. Lee, A. S. T. Tan, D. Ishak, and R. Mohd-Mokhtar, "Single-phase simplified split-source inverter (S3I) for boost DC–AC power conversion," *IEEE Trans. Ind. Electron.*, vol. 66, no. 10, pp. 7643–7652, Oct. 2019.

[11] O. Ray and S. Mishra, "Boost-derived hybrid converter with simultaneous DC and AC outputs," *IEEE Trans. Ind. Appl.*, vol. 50, no. 2, pp. 1082–1093, Mar. 2014.

[12] S. Dey, V. K. Bussa, and R. K. Singh, "Transformerless hybrid converter with AC and DC outputs and reduced leakage current," *IEEE J. Emerg. Sel. Top. Power Electron.*, vol. 7, no. 2, pp. 1329–1341, Jun. 2019.

[13] Z. Tang, Y. Yang, M. Su, H. Han, and F. Blaabjerg, "A symmetrical transformerless hybrid converter with leakage current suppression," in *Prof. of ECCE*, Sep. 2019, pp. 6680–6685.

[14] Z. Tang, Y. Yang, M. Su, T. Jiang, F. Blaabjerg, H. Dan, and X. Liang, "Modulation for the AVC-HERIC inverter to compensate for deadtime and minimum pulsewidth limitation distortions," *IEEE Trans. Power Electron.*, vol. 35, no. 3, pp. 2571–2584, Mar. 2020.

[15] S. Heribert, S. Christoph, and K. Jurgen, "Inverter for transforming a DC voltage into an AC current or an AC voltage," Europe Patent 1 369 985 (A2), May, 2003.

[16] K. Li, Y. Shen, Y. Yang, Z. Qin, and F. Blaabjerg, "A transformerless single-phase symmetrical Z-source HERIC inverter with reduced leakage currents for PV systems," in *Proc. of APEC*, Mar. 2018, pp. 356–361.

[17] B. Axelrod, Y. Berkovich, and A. Ioinovici, "Switched-capacitor/switched-inductor structures for getting transformerless hybrid DC–DC PWM converters," *IEEE Trans. Circuits Syst. I, Reg. Papers*, vol. 55, no. 2, pp. 687–696, Mar. 2008.